Order and disorder in Ni_3V: Effective pair interactions and the role of electronic excitations

M. Barrachin
Office National d'Etudes et de Recherches Aérospatiales (ONERA), Boîte Postale 72, 92322 Châtillon Cédex, France and Laboratoire Léon Brillouin (CEA-CNRS), Centre d'Etudes Nucléaires de Saclay, 91191 Gif-sur-Yvette Cédex, France

A. Finel
Office National d'Etudes et de Recherches Aérospatiales (ONERA), Boîte Postale 72, 92322 Châtillon Cédex, France

R. Caudron
Office National d'Etudes et de Recherches Aérospatiales (ONERA), Boîte Postale 72, 92322 Châtillon Cédex, France and Laboratoire Léon Brillouin (CEA-CNRS), Centre d'Etudes Nucléaires de Saclay, 91191 Gif-sur-Yvette Cédex, France

A. Pasturel
Laboratoire de Thermodynamique et Physico-Chimie Metallurgiques Ecole Nationale Supérieure d'Electronique et d'Electromécanique de Grenoble, Boîte Postale 75, 38402 St. Martin d'Heres Cédex, France

A. Francois
Laboratoire d'Etude des Microstructures (UMR 104 CNRS), ONERA, Boîte Postale 72, 92322 Châtillon Cédex, France
(Received 26 July 1994)

In situ neutron diffuse scattering experiments were performed on disordered Ni_3V. Effective pair interactions (EPI) were deduced from the measured short-range order parameters. The EPI were used to predict successfully the disordering temperature and the temperature dependence of the excess free energies of two different antiphases in the ordered phase. We also computed the energy difference between DO_{22} and $L1_2$: our result is eight times lower than found by electronic structure calculations at 0 K. This discrepancy is partly due to electronic excitations.

Many theoretical studies have shown that the thermodynamics of a substitutional binary alloy A_cB_{1-c} may be described by a generalized Ising Hamiltonian,

$$H=\frac{1}{2}\sum_{n,m}J_{nm}(\sigma_n-\sigma)(\sigma_m-\sigma)+\cdots , \tag{1}$$

where the J_n's are the effective pair interactions (EPI) and the σ_n's are pseudospin variables ($\sigma_n=+1$ or -1 depending on whether or not site n is occupied by an A species), and where σ is the mean value of σ_n on all the lattice sites ($\sigma=2c-1$). This form for H is a result of the generalized perturbation method.[1,2] H represents the difference between the total energy of a given configuration $\{\sigma_n,\sigma_m\cdots\}$ and the energy $E_{\rm dis}(c)$ of the totally disordered alloy.

We will show how a set of effective pair interactions has been deduced from *in situ* diffuse scattering of neutrons in the *disordered* state, and used to predict correctly not only the transition temperature Ni_3V, but also the values and the temperature variations of the dissociation width of superdislocations in the *ordered* state. This stringent test of the model gives us confidence in its parameters and leads us to compare them with results of first-principles electronic structure calculations: with our model, we can compute an energy difference between the DO_{22} and the $L1_2$ structures which strongly contradicts the value yielded by linear muffin-tin orbital–atomic-sphere approximation (LMTO–ASA) (Refs. 3–5 and present work) and linear augmented plane-wave[6] (LAPW) calculations. We show that this discrepancy is partly due to the difference of electronic free energy between DO_{22} and $L1_2$.

The EPI have been deduced from diffuse scattering experiments in the disordered phase: the diffuse intensity is a modulation of the Laue intensity $c(1-c)(b_A-b_B)^2$ by the Fourier transform $\alpha(q)$ of the short-range order (SRO) parameters

$$\alpha(R)=\{\langle\sigma_O\sigma_R\rangle-\langle\sigma_O\rangle\langle\sigma_R\rangle\}/4c(1-c) ,$$

where the brackets denote thermodynamic averages and where R is a lattice vector with respect to some origin O.

Ni_3V has been investigated *in situ* at 1100 °C in a dedicated spectrometer[7] located at LLB. The elastic intensities were submitted to a least-squares fitting procedure, using 10–25 $\alpha(R)$ and first-order displacement parameters. We present in Fig. 1 the diffuse intensity $\alpha(q)$.

The short-range-order parameters were then used to deduce the EPI. A previous investigation using an inverse cluster variation method (ICVM),[8] limited to the first four EPI,[9,10] led to the results displayed in the first column of Table I. The diffuse intensity map, simulated by Monte Carlo (MC) with these four interactions, is displayed in Fig. 2. The overall shape of the experimental map is correctly reproduced, but the calculated maxima are more elongated along $(1\zeta 0)$ and weaker than for the experiment.

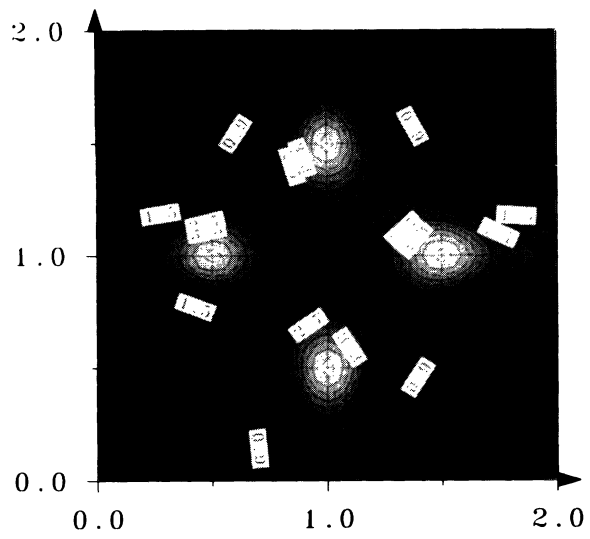

FIG. 1. Experimental diffuse intensity $\alpha(q)$ in Ni_3V at $T=1100\,^{\circ}C$ in the $\langle 100 \rangle$ plane (Laue units).

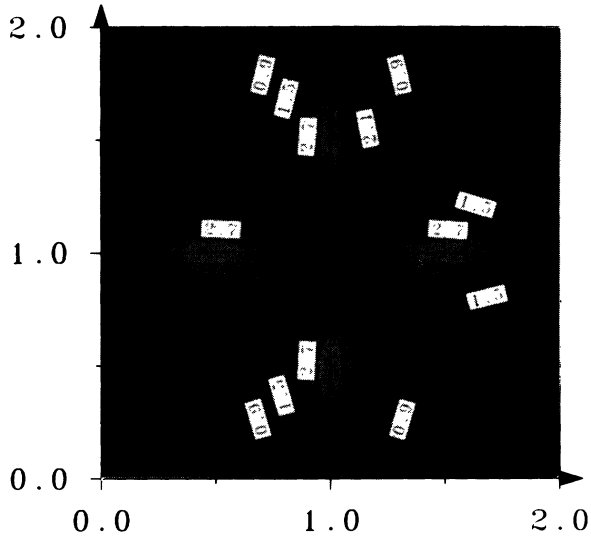

FIG. 2. Calculated diffuse intensity $\alpha(q)$ at $T=1100\,^{\circ}C$ in the $\langle 100 \rangle$ plane, using four interactions (second column of Table I) (Laue units).

In order to investigate longer-ranged interactions, we have developed an inverse Monte Carlo (IMC) code,[10,11] based on the general trial and error algorithm already used in our ICVM. In a first step, we have checked (Table I) that the first four EPI obtained by IMC were the same as by ICVM. In a second step, we have selected all the EPI up to J_9 and used the corresponding short-range-order parameters. The results are shown in the third column of Table I. Finally, in order to check the relevance of the EPI J_5 to J_9 we tried to suppress them, one by one and used again the IMC with these reduced sets, but keeping all the SRO parameters up to the ninth neighbors. The criteria used to select an interaction set are the convergence of the IMC and the faithfulness of the diffuse intensity map computed by using the output of the inverse algorithm as an input of a direct MC simulation.

Our best set is displayed in the last column of Table I. The corresponding intensity map (Fig. 3) is very close to the experimental one (Fig. 1), particularly for the amplitudes and the shape of the intensity maxima [Table I displays the values of the calculated and experimental maxima $\alpha(q=1\frac{1}{2}0)$].

These EPI can be used to predict other physical properties. The comparison of the predicted quantities to those from other experimental fields will be a test of the validity and transferability of our interactions.

TABLE I. Effective pair interactions in Ni_3V for different sets of EPI (see text). An * means an interaction not used in the inverse algorithm. α_{max} is the calculated diffuse intensity maximum, i.e., $\alpha(q=1\frac{1}{2}0)$ (Laue units). T_C is the calculated ordering temperature of the DO_{22} phase. ΔE is the energy difference, per atom, between DO_{22} and $L1_2$, as defined in (3). $\xi(100)$ and $\xi(111)$ are the energies of the conservative antiphases in the (100) and (111) planes [per site of the antiphase plane, see (2)]. Experimental data are given in square brackets and error bars in parentheses; same units.

	Inverse CVM	Inverse Monte Carlo		
		Four potentials	Full set	Best set
J_1	35 (5)	34.4 (5)	34.3 (2)	36.2 (2)
J_2	−10 (3)	−10.2 (3)	−8.4 (2)	−7.8 (2)
J_3	−1.5 (2)	−1.5 (1)	−2.5 (0.5)	−0.5 (0.5)
J_4	4 (2)	4.0 (2)	0.9 (1)	3.5 (0.7)
J_5	*	*	−0.7 (1)	*
J_6	*	*	−0.9 (1)	*
J_7	*	*	−1.3 (0.5)	−0.5 (0.2)
J_8	*	*	−2.8 (0.7)	−2.4 (0.3)
J_9	*	*	−2.0 (0.7)	−1.5 (0.2)
α_{max} [exp: 4.3]		3.5	4.7	4.3
T_C [exp: 1045 °C]	730 °C	735 °C	850 °C	840 °C
ΔE ($DO_{22}-L1_2$)	−12 (5)	−12 (5)	−12 (2)	−12 (2)
$\xi(100)$ [exp: 50(10)]	24 (10)	24 (11)	36 (4)	34 (5)
$\xi(111)$ [exp: 75(15)]	59 (2)	59 (2)	75 (3)	72 (4)

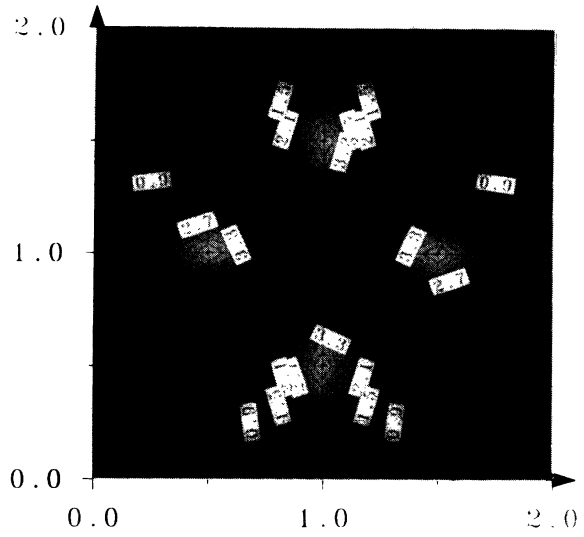

FIG. 3. Calculated diffuse intensity $\alpha(q)$ at $T=1100\,^{\circ}\mathrm{C}$ in the $\langle 100\rangle$ plane, using our optimal interaction set (last column of Table I) (Laue units).

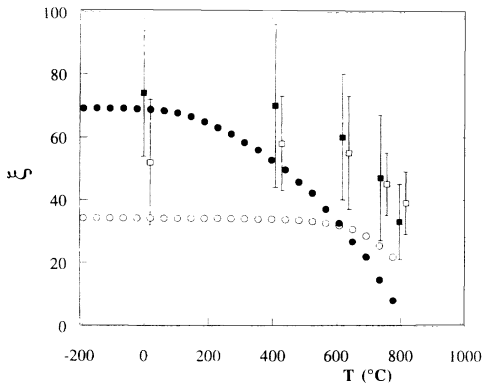

FIG. 4. Free energies of the (100) (empty symbols) and (111) (solid symbols) antiphases in the DO_{22} phase, as functions of temperature. The circles represent the Monte Carlo calculations using our optimal interaction set (last column of Table I); the squares are the experimental data with their error bars (energy units: meV/atom).

First, by MC simulations, we have calculated the transition temperature T_C between the disordered phase and the DO_{22} compound, which is the stable low-temperature phase of Ni_3V. The results are reported in Table I. They are in reasonable agreement with the experimental T_C.

A much more stringent test of the transferability of the EPI issued from our measurements in the *disordered* state is to use them to compute antiphase energies in the *ordered* state and to compare the computed values to those obtained experimentally through a study of the dissociation length of superdislocations in the DO_{22} phase.[12] The excess energies of the conservative antiphase boundaries in the (100) and (111) planes of the DO_{22} phase[13] are given by (per site of the antiphase plane):

$$\xi(100)=2J_2-8J_3+8J_4+8J_6-16J_7-4J_8\ , \tag{2a}$$

$$\xi(111)=J_1-J_2-4J_3+2J_4+6J_5+6J_6 -12J_7-6J_8+3J_9\ . \tag{2b}$$

Their numerical estimates, based on our optimal interactions set, are displayed in Table I.

The experimental values[12] have been deduced[14] from the measurement of the dissociation width of dislocations in samples deformed *in situ* at various temperatures, by transmission electron microscopy (weak beam technique). The experimental values, extrapolated at 0 K, are displayed in Table I: the agreement with our computed value is excellent, in particular for the (111) antiphase.

A finite temperature, when entropy effects are no more negligible, the dissociation lengths are governed by the free energies of the antiphases. We have computed these free energies through MC simulations, with appropriate boundary conditions, and with our optimal interaction set (last column of Table I). The results are shown in Fig. 4, along with the experimental data. The agreement is again very good.

Now, we can safely discuss our results in relation to electronic structure calculations. Up to now, no reliable calculation of individual EPI is available for Ni_3V, but quantities which can easily be related to our EPI have been calculated: the energy difference $\Delta E=E(DO_{22})-E(L1_2)$ in Ni_3V has been investigated using the LMTO-ASA (Refs. 3–5 and present work) and the full potential-augmented plane-wave[6] (FP-APW) methods. The results are reported in Table II. All these studies lead to the same $\Delta E\approx -100$ meV/atom, in agreement with the observed stability of DO_{22}.

In our model, ΔE, which is close to half the opposite of the antiphase energy $\xi(100)$ (2a), is given by

$$\Delta E=-J_2+4J_3-4J_4-4J_6+8J_7\ . \tag{3}$$

Numerical values, evaluated for each interaction set, are displayed in Table I: all of them are negative, also in agreement with the stability of DO_{22}. We also note that they are almost the same for all the interaction sets: the average value ($\Delta E\approx -12$ meV/atom) is displayed in Table II, together with its error bar. It is in strong disagreement with the theoretical results.

This discrepancy could be due to the elastic effects, as our EPI are extracted from experimental observations in the disordered phase, which does not *a priori* exhibit the same elastic relaxations as the ordered $L1_2$ and DO_{22} compounds. But this is not the case, for the following reasons: (1) the lattice distortions in the disordered phase are small, as indicated by the small deviation from periodicity in the experimental intensity maps;[9] (2) the lattice parameter change on ordering is small ($<1\%$); (3) the *ab initio* calculations mentioned above lead to the same ΔE, whether or not the volume relaxation in $L1_2$ and DO_{22} is taken into account (see for instance Fig. 3 of Ref. 4, where the curves of the total energies of the two

TABLE II. Energy difference ΔE between DO_{22} and $L1_2$ in Ni_3V (meV/atom). Comparison between electronic structure calculations and the experimental determination.

	Electronic structure calculations					Experiment
ΔE	−109	−95	−108	−100	−100	−12 (5)
	[Ref. 3]	[Ref. 4]	[Ref. 5]	[Ref. 6]	(our work)	

compounds as a function of the lattice spacing are parallel to each other); (4) ΔE is not sensitive to the tetragonal relaxation in DO_{22}, as the authors taking those effects into account[3] find the same results as those who do not.[4]

It might also be argued that the choice of the EPI believed to significant and used in the IMC is arbitrary: different sets of selected interactions might satisfy the procedure and yield the same simulated intensity maps. This point has been discussed above, and our choice yields the best maps. We also notice that we get almost the same ΔE with all the sets of EPI selected above (see Table I). Moreover, the order of magnitude of ΔE can be read directly on the experimental diffuse intensity maps, independently of any interaction set, using the approximate Krivoglaz-Clapp-Moss (KCM) formula.[15] By this method,[16] we obtain $\Delta E \approx -10$ meV.

Concerning the antiphase energies $\xi(100)$ and $\xi(111)$, we have seen above that their values and their behaviors are correctly predicted by our model (see Fig. 4) This gives us extra confidence in our model.

We have finally concluded that our results for the energy difference and the antiphase energies were soundly established, and that the results of the electronic structure calculations need to be revisited: a gradient expansion of the otherwise local contribution of the exchange energy[17] does not modify significantly ΔE, nor does a calculation performed without any shape approximation for the potential and the charge density (full potential LMTO). The conclusion of these new calculations is that no obvious source of error shows up for the theoretical value of ΔE itself.

At this step, it must be noticed that our EPI have been deduced from measurements performed around 1400 K. At this temperature, excitations are important. Of course, the configurational entropy S_c and energy have been explicitly accounted for (this is the very nature of our inverse procedures). However, the order of magnitude of the other excitation terms must be evaluated, in order to know to what extent they could bias the EPI. The vibrational free energy difference between $L1_2$ and DO_{22} amounts to a few meV only, but, as shown below, the difference ΔF_e of electronic free energy F_e is sizeable.

Taking F_e into account, the true free energy of the system is

$$F = E + F_e - TS_c = \frac{1}{2}\sum_{n,m} J_{nm}\langle \sigma_n \sigma_m \rangle + F_e - TS_c \ , \qquad (4)$$

whereas we have chosen the set of $\tilde{J}_{nm}$ such that the experimental correlation functions minimize:

$$\tilde{F} = \tilde{E} - TS_c = \frac{1}{2}\sum_{n,m} \tilde{J}_{nm}\langle \sigma_n \sigma_m \rangle - TS_c \ . \qquad (5)$$

Of course, the $\tilde{J}$'s differ from the true J's; in particular, they are temperature dependent. However, since the $\tilde{J}$'s have been obtained by forcing the model to fit the situation at 1400 K, Eq. (5) is a rough approximation of Eq. (4) at temperature close to 1400 K and for configurations which, like $L1_2$ or DO_{22}, are not too far from the local order present at 1400 K. Thus, using (3) with our set of $\tilde{J}$'s, we have, instead of the true ΔE, estimated $\Delta\tilde{E} = \tilde{E}(DO_{22}) - \tilde{E}(L1_2) = -12$ meV, which is just the difference $\Delta E + \Delta F_e$ between DO_{22} and $L1_2$ at 1400 K. Hence, in order to obtain the theoretical counterpart of this experimental quantity, we must add $\Delta F_e = F_e(DO_{22}) - F_e(L1_2)$ to ΔE. As the density of states at the Fermi level $n(E_F)$ of Ni_3V in the DO_{22} structure is about 30 Ryd^{-1} per cell (or 0.55 eV^{-1}/atom), to be compared with 170 (or 3.13) for $L1_2$, $\Delta F_e = -\pi^2 \Delta n(E_F)(k_B T)^{2/6}$ (Ref. 18) amounts to about 60 meV at 1400 K. It improves considerably the agreement with the low value we found experimentally for $\Delta\tilde{E}$.

To summarize, we have shown, that for Ni_3V, EPI can be deduced from diffuse scattering in the *disordered* state. We used them to predict successfully the transition temperature and the dissociation widths of dislocations, which are properties of the *ordered* phase. However, the computed value of the energy difference between DO_{22} and $L1_2$ is eight times lower than found by electronic structure calculations at 0 K. This discrepancy is partially explained by the electronic excitations.

[1] F. Ducastelle and F. Gautier, J. Phys. F **6**, 2039 (1976).

[2] F. Ducastelle, in *Order and Phase Stability in Alloys,* edited by F. R. de Boer and D. G. Pettifor, Cohesion and Structure Vol. 3 (North-Holland, Amsterdam, 1991).

[3] J. H. Xu, T. Oguchi, and A. J. Freeman, Phys. Rev. B **35**, 6940 (1987).

[4] S. Pei *et al.*, Phys. Rev. B **39**, 5767 (1989).

[5] W. Lin, J. H. Xu, and A. J. Freeman, Phys. Rev. B **45**, 10 863 (1992).

[6] A. Zunger (private communication).

[7] R. Caudron *et al.*, J. Phys. I (France) **2**, 1145 (1992).

[8] A. Finel, in *Statics and Dynamics of Alloy Phase Transformation,* edited by A. Gonis and P. E. A. Turchi (Plenum, New York, 1993), p. 495.

[9] R. Caudron *et al.*, in *Statics and Dynamics of Alloy Phase Transformations,* (Ref. 8), p. 171.

[10] M. Barrachin, Ph.D. Paris XI, 1993.

[11] F. Livet, Acta Metall. **35**, 2915 (1987).

[12] A. François, Ph.D. Paris VI, 1992.

[13] If the last index refers to the tetragonal axis, these antiphases correspond to a $\frac{1}{2}(110)$ shear of one half of the crystal. The energies are given per site of the antiphase plane.

[14] J. Douin, P. Veyssière, and P. Beauchamp, Philos. Mag. A **54**, 375 (1986).

[15] M. A. Krivoglaz and A. A. Smirnov, *The Theory of Order and Disorder in Alloys* (McDonald, London, 1964); P. C. Clapp and S. C. Moss, Phys. Rev. **142**, 418 (1966).

[16] The KCM formula gives $\alpha(q) = [1 + 4\beta c(1-c)J(q)]^{-1}$, where $J(q)$ is the Fourier transform of the EPI. The difference between the inverses of $\alpha(q)$ at q_1 and q_2 can be written: $\Delta\alpha^{-1}(q_1,q_2) = \alpha^{-1}(q_1) - \alpha^{-1}(q_2) = 4c(1-c)\beta[J(q_1) - J(q_2)]$. With $q_1 = (100)$ and $q_2(1\frac{1}{2}0)$, we obtain $\Delta\alpha^{-1}[(100),(1\frac{1}{2}0)] = -16c(1-c)\beta\Delta E$, where ΔE is given by (5).

[17] D. C. Langreth and M. J. Mehl, Phys. Rev. B **28**, 1809 (1983).

[18] This expression is valid for smooth density of state curves at E_F. This is not necessarily the case for the transition metals and their alloys.

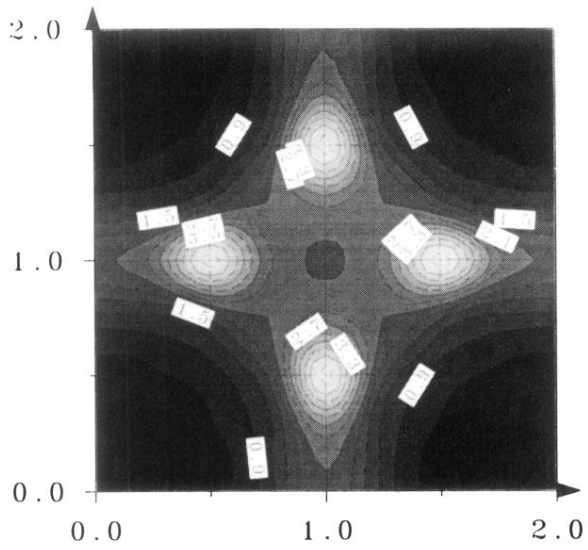

FIG. 1. Experimental diffuse intensity $\alpha(q)$ in Ni_3V at $T = 1100\,^{\circ}C$ in the $\langle 100 \rangle$ plane (Laue units).

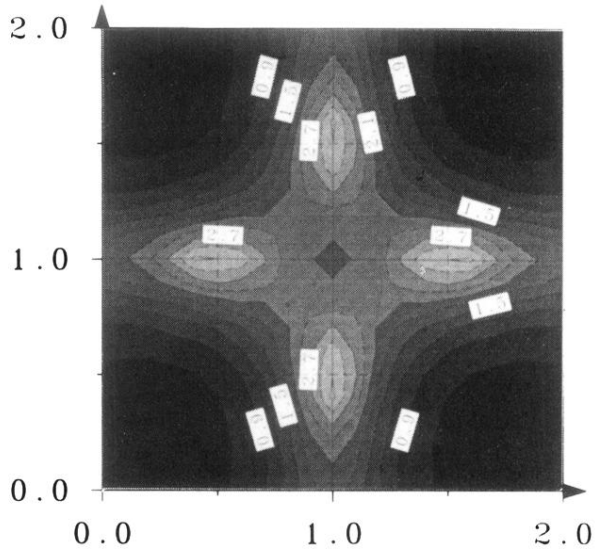

FIG. 2. Calculated diffuse intensity $\alpha(q)$ at $T = 1100\,^{\circ}\mathrm{C}$ in the $\langle 100 \rangle$ plane, using four interactions (second column of Table I) (Laue units).

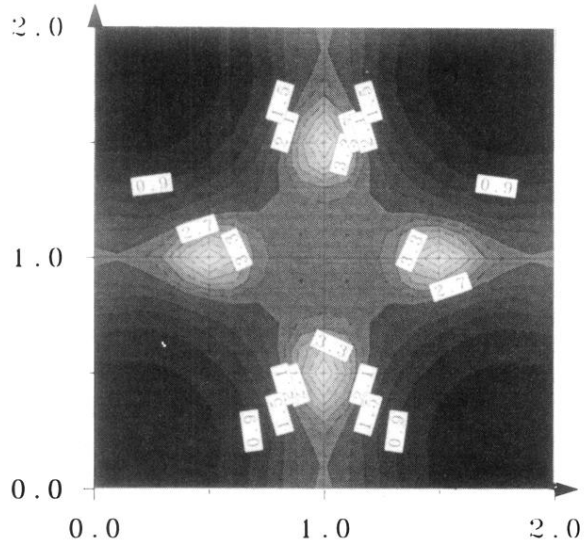

FIG. 3. Calculated diffuse intensity $\alpha(q)$ at $T = 1100\,^{\circ}\mathrm{C}$ in the $\langle 100 \rangle$ plane, using our optimal interaction set (last column of Table I) (Laue units).